J|A|C|S ARTICLES

Published on Web 10/28/2010

Water-Soluble Organo−Silica Hybrid Nanotubes Templated by Cylindrical Polymer Brushes

Markus Müllner, Jiayin Yuan, Stephan Weiss, Andreas Walther, Melanie Förtsch, Markus Drechsler, and Axel H. E. Müller*

Makromolekulare Chemie II, Universität Bayreuth, D-95440 Bayreuth, Germany

Received August 9, 2010; E-mail: axel.mueller@uni-bayreuth.de

Abstract: We report the preparation of water-soluble organo−silica hybrid nanotubes templated by core−shell−corona structured triblock terpolymer cylindrical polymer brushes (CPBs). The CPBs consist of a polymethacrylate backbone, a poly(*tert*-butyl acrylate) (P*t*BA) core, a poly(3-(trimethoxysilyl)propyl acrylate) (PAPTS) shell, and a poly(oligo(ethylene glycol) methacrylate) (POEGMA) corona. They were prepared via the "grafting from" strategy by the combination of two living/controlled polymerization techniques: anionic polymerization for the backbone and atom transfer radical polymerization (ATRP) for the triblock terpolymer side chains. The monomers *t*BA, APTS, and OEGMA were consecutively grown from the pendant ATRP initiating groups along the backbone to spatially organize the silica precursor, the trimethoxysilyl groups, into a tubular manner. The synthesized core−shell−corona structured CPBs then served as a unimolecular cylindrical template for the in situ fabrication of water-soluble organo−silica hybrid nanotubes via base-catalyzed condensation of the PAPTS shell block. The formed tubular nanostructures were characterized by transmission electron microscopy (TEM), cryogenic TEM, and atomic force microscopy.

Introduction

Cylindrical polymer brushes (CPBs) or "molecular bottlebrushes", which possess linear side chains or high-generation dendritic side groups densely grafted from a linear main chain, have been the research focus of many polymer chemists and theoreticians over the past decade.[1,2] The interest in this unique hierarchical polymeric architecture arises from the fact that the extended, wormlike chain conformation enables single macromolecular visualization and manipulation, and that particular behavior in solution and bulk has been observed in such macromolecules. So far, three major strategies have been involved in the preparation of CPBs: the "grafting through",[3] "grafting onto",[4] and "grafting from"[5] strategies. As compared to the first two mechanisms, "grafting from" has drawn more attention as an effective pathway to prepare CPBs of precise dimension and desired functionality. In this approach, a relatively long backbone is first prepared via a living/controlled polymerization technique. This is followed by attaching initiating sites onto each repeating unit along the backbone. Side chains are then grown from these pendant initiating sites, which introduce steric repulsion and lead to stretching of the backbone. Applying the "grafting from" strategy in the field of CPBs has been greatly promoted by the recent progress in living/controlled polymerization techniques, like atom transfer radical polymerization (ATRP),[6,7] nitroxide-mediated radical polymerization,[8] and ring-opening polymerization.[9,10] Such techniques have made it possible and convenient to grow uniform side chains with defined chemical structures and compositions. Among them, as a very efficient living/controlled radical polymerization technique, ATRP shows excellent tolerance to many functional groups in monomers and has been widely employed to graft various side chains from the CPB backbone. Another unique advantage of ATRP when used in the "grafting from" strategy is that block copolymer side chains can be stepwise introduced for the construction of more complex architecture. On the basis of this technique, CPBs with various architectures have been prepared, including homopolymer brushes,[11,12] core−shell CPBs,[6,13−16] core−shell−corona CPBs,[17,18] heterografted

(1) Sheiko, S. S.; Sumerlin, B. S.; Matyjaszewski, K. *Prog. Polym. Sci.* **2008**, *33*, 759–785.
(2) Zhang, M.; Müller, A. H. E. *J. Polym. Sci., Part A: Polym. Chem.* **2005**, *16*, 3461–3481.
(3) Tsukahara, Y.; Mizuno, K.; Segawa, A.; Yamashita, Y. *Macromolecules* **1989**, *22*, 1546–1552.
(4) Deffieux, A.; Schappacher, M. *Macromolecules* **1999**, *32*, 1797–1802.
(5) Qin, S.; Matyjaszewski, K.; Xu, H.; Sheiko, S. S. *Macromolecules* **2003**, *36*, 605–612.
(6) Cheng, G.; Böker, A.; Zhang, M.; Krausch, G.; Müller, A. H. E. *Macromolecules* **2001**, *34*, 6883–6888.
(7) Beers, K. L.; Gaynor, S. G.; Matyjaszewski, K.; Sheiko, S. S.; Möller, M. *Macromolecules* **1998**, *31*, 9413–9415.
(8) Cheng, C.; Qi, K.; Khoshdel, E.; Wooley, K. L. *J. Am. Chem. Soc.* **2006**, *128*, 6808–6809.
(9) Lee, H.-i.; Jakubowski, W.; Matyjaszewski, K.; Yu, S.; Sheiko, S. S. *Macromolecules* **2006**, *39*, 4983–4989.
(10) Lee, H.-i.; Matyjaszewski, K.; Yu-Su, S.; Sheiko, S. S. *Macromolecules* **2008**, *41*, 6073–6080.
(11) Li, C.; Gunari, N.; Fischer, K.; Janshoff, A.; Schmidt, M. *Angew. Chem., Int. Ed.* **2004**, *43*, 1101–1104.
(12) Xu, Y.; Bolisetty, S.; Drechsler, M.; Fang, B.; Yuan, J.; Ballauff, M.; Müller, A. H. E. *Polymer* **2008**, *49*, 3957–3964.
(13) Zhang, M.; Breiner, T.; Mori, H.; Müller, A. H. E. *Polymer* **2003**, *44*, 1449–1458.
(14) Djalali, R.; Hugenberg, N.; Fischer, K.; Schmidt, M. *Macromol. Rapid Commun.* **1999**, *20*, 444–449.
(15) Börner, H. G.; Beers, K.; Matyjaszewski, K.; Sheiko, S. S.; Möller, M. *Macromolecules* **2001**, *34*, 4375–4383.
(16) Ishizu, K.; Kakinuma, H. *J. Polym. Sci., Part A: Polym. Chem.* **2005**, *43*, 63–70.

brushes,[19] brush block copolymers,[10,20] star brushes,[21,22] and double-grafted brushes.[23,24] The functional polymerizable monomers in ATRP render CPBs responsive to stimuli such as solvent,[25] temperature,[11,26] light,[27] pH,[12] and salts.[12]

The wormlike shape of CPBs has been employed to fabricate inorganic one-dimensional (1D) nanostructures,[28] such as γ-Fe_2O_3,[29] CdS,[30] CdSe,[31] Au,[32] and titania[33] nanowires. Commonly, in a solution approach, the inorganic precursors have been first localized in the cylindrical core area by selectively interacting with the CPB core block. Through chemical reactions occurring only within the core, the precursors have been converted into corresponding functional inorganic nanomaterials, which were spatially organized by the cylindrical template to adopt a wire-like geometry. The CPB shell, free of interaction with the inorganic moieties, protects the formed inorganic nanowires from agglomeration and solubilizes them in solvents. Solubility in water or organic solvents and biocompatibility of the hybrid nanowires can be achieved by the design of the shell block.[33,34] Freestanding, purely inorganic nanowires can be achieved by pyrolytic removal of the polymeric template on a solid substrate. In general, the dimensions of the desired 1D inorganic nanostructure are strictly controlled by the CPBs. For example, the diameter depends on the length of the block in the CPB core, and the length is largely determined by the degree of polymerization of the backbone.[34] We recently reported a novel strategy to form hybrid cylinders with an organo-silica core, where the precursor for the inorganic part is a building unit of the core itself.[34] Organo−silica hybrid nanowires were produced by using poly[(3-acryloxypropyl) trimethoxysilane)] (PAPTS) as the core and poly[oligo(ethylene glycol) methacrylate] (POEGMA) as the corona, followed by hydrolytic condensation of the PAPTS core block to form a crosslinked silsesquioxane structure, which could be pyrolized to form pure silica nanowires.[35] Cylindrical or tubular hybrid materials that are not derived from CPBs have been synthesized by using block copolymers as directing agents.[18,36]

So far, only core−shell structured CPBs with diblock copolymer side chains have been chosen as synthetic 1D templates. Herein, we demonstrate the first time that core−shell−corona structured CPBs with triblock terpolymer side chains are employed as an in situ template for the construction of organo−silica hybrid nanotubes, which are soluble in various solvents. First, block terpolymer side chains of poly(*tert*-butyl acrylate)-*block*-PAPTS-*block*-POEGMA were grown from a poly(2-(2-bromoisobutyryloxy)ethyl methacrylate) (PBIEM) polyinitiator backbone via ATRP. They were then used as a unimolecular cylindrical template for the in situ fabrication of water-soluble organo−silica hybrid nanotubes via condensation of the PAPTS shell block. The formed tubular structures were characterized by transmission electron microscopy (TEM), cryogenic TEM (cryo-TEM), and atomic force microsopy (AFM). Soft tubular nanostructures have also been prepared from small surfactants[37,38] amphiphilic block copolymers,[39−43] or multicomponent copolymer cylindrical brushes.[44,45] However, most of these conventional tubular structures are only dynamically stable and can collapse upon a tiny perturbation in the external environment such as a solvent, temperature, concentration, or pH change. In addition, the size and size distribution of assembled structures are usually hard to control. In contrast, due to the living/controlled polymerization techniques employed in the preparation of CPBs, the obtained hybrid tubular structures are uniform in diameter and length. They are stable and tolerant to variations in their environment because the shape and structure of each nanotube are covalently locked.

Experimental Section

Materials. All chemicals were of analytical grade and used as received without further purification, except that (3-acryloxypropyl)trimethoxysilane (APTS) (95%, ABCR) was freshly distilled, and *tert*-butyl acrylate (*t*BA) (98%, Aldrich) and oligo(ethylene glycol) methacrylate (OEGMA) (98%, Aldrich) were filtered through a basic alumina column shortly before each polymerization.

Preparation of Core−Shell−Corona CPB [tBA$_{75}$-APTS$_{115}$-OEGMA$_{150}$]$_{3200}$. The poly(macroinitiator) backbone poly(2-(2-bromoisobutyryloxy)ethyl methacrylate) (PBIEM) was prepared by anionic polymerization of 2-(trimethysilyloxy)ethyl methacrylate, acidic cleavage of the trimethylsilyl groups, and an esterification reaction to attach the ATRP initiating sites onto each repeating unit as detailed earlier.[13] The degree of polymerization (DP) of the PBIEM polyinitiator backbone is 3200, and its polydispersity index, determined by gel permeation chromatography (GPC), is 1.14. The synthesis of a P*t*BA homopolymer CPB in anisole was detailed in

(17) Tang, C.; Dufour, B.; Kowalewski, T.; Matyjaszewski, K. *Macromolecules* **2007**, *40*, 6199–6205.
(18) Zhang, K.; Gao, L.; Chen, Y. *Polymer* **2010**, *51*, 2809–2817.
(19) Neugebauer, D.; Zhang, Y.; Pakula, T.; Matyjaszewski, K. *Polymer* **2003**, *44*, 6863–6871.
(20) Ishizu, K.; Satoh, J.; Sogabe, A. *J. Colloid Interface Sci.* **2004**, *274*, 472–479.
(21) Lee, H.-i.; Boyce, J. R.; Nese, A.; Sheiko, S. S.; Matyjaszewski, K. *Polymer* **2008**, *49*, 5490–5496.
(22) Matyjaszewski, K.; Qin, S.; Boyce, J. R.; Shirvanyants, D.; Sheiko, S. S. *Macromolecules* **2003**, *36*, 1843–1849.
(23) Neugebauer, D.; Zhang, Y.; Pakula, T.; Sheiko, S. S.; Matyjaszewski, K. *Macromolecules* **2003**, *36*, 6746–6755.
(24) Xu, Y.; Becker, H.; Yuan, J.; Burkhardt, M.; Zhang, Y.; Walther, A.; Bolisetty, S.; Ballauff, M.; Müller, A. H. E. *Macromol. Chem. Phys.* **2007**, *208*, 1666–1675.
(25) Fischer, K.; Schmidt, M. *Macromol. Rapid Commun.* **2001**, *22*, 787–791.
(26) Pietrasik, J.; Sumerlin, B.; Lee, R.; Matyjaszewski, K. *Macromol. Chem. Phys.* **2007**, *208*, 30–36.
(27) Lee, H.-i.; Pietrasik, J.; Matyjaszewski, K. *Macromolecules* **2006**, *39*, 3914–3920.
(28) Yuan, J.; Müller, A. H. E. *Polymer* **2010**, *51*, 4015–4036.
(29) Zhang, M.; Estournès, C.; Bietsch, W.; Müller, A. H. E. *Adv. Funct. Mater.* **2004**, *14*, 871–882.
(30) Zhang, M.; Drechsler, M.; Müller, A. H. E. *Chem. Mater.* **2004**, *16*, 537–543.
(31) Yuan, J.; Drechsler, M.; Xu, Y.; Zhang, M.; Müller, A. H. E. *Polymer* **2008**, *49*, 1547–1554.
(32) Djalali, R.; Li, S.-Y.; Schmidt, M. *Macromolecules* **2002**, *35*, 4282–4288.
(33) Yuan, J.; Lu, Y.; Schacher, F.; Lunkenbein, T.; Weiss, S.; Schmalz, H.; Müller, A. H. E. *Chem. Mater.* **2009**, *21*, 4146–4154.
(34) Yuan, J.; Xu, Y.; Walther, A.; Bolisetty, S.; Schumacher, M.; Schmalz, H.; Ballauff, M.; Müller, A. H. E. *Nat. Mater.* **2008**, *7*, 718–722.
(35) Yuan, J.; Schacher, F.; Drechsler, M.; Hanisch, A.; Lu, Y.; Ballauff, M.; Müller, A. H. E. *Chem. Mater.* **2010**, *22*, 2626–2634.
(36) Jain, A.; Wiesner, U. *Macromolecules* **2004**, *37*, 5665–5670.
(37) Zhai, L.; Herzog, B.; Drechsler, M.; Hoffmann, H. *J. Phys. Chem. B* **2006**, *110*, 17697–17701.
(38) Grabner, D.; Zhai, L.; Talmon, Y.; Schmidt, J.; Freiberger, N.; Glatter, O.; Herzog, B.; Hoffmann, H. *J. Phys. Chem. B* **2008**, *112*, 2901–2908.
(39) Kuo, S.-W.; Lee, H.-F.; Huang, C.-F.; Huang, C.-J.; Chang, F.-C. *J. Polym. Sci., Part A: Polym. Chem.* **2008**, *46*, 3108–3119.
(40) Yan, D.; Zhou, Y.; Hou, J. *Science* **2004**, *303*, 65–67.
(41) Raez, J.; Manners, I.; Winnik, M. A. *J. Am. Chem. Soc.* **2002**, *124*, 10381–10395.
(42) Yu, K.; Eisenberg, A. *Macromolecules* **1998**, *31*, 3509–3518.
(43) Liu, G. *Adv. Polym. Sci.* **2008**, *220*, 29–64.
(44) Huang, K.; Rzayev, J. *J. Am. Chem. Soc.* **2009**, *131*, 6880–6885.
(45) Huang, K.; Canterbury, D. P.; Rzayev, J. *Macromolecules* **2010**, *43*, 6632–6638.

Scheme 1. Synthetic Route To Obtain Water-Soluble Organo−Silica Hybrid Nanotubes Templated by Core−Shell−Corona Structured CPBs[a]

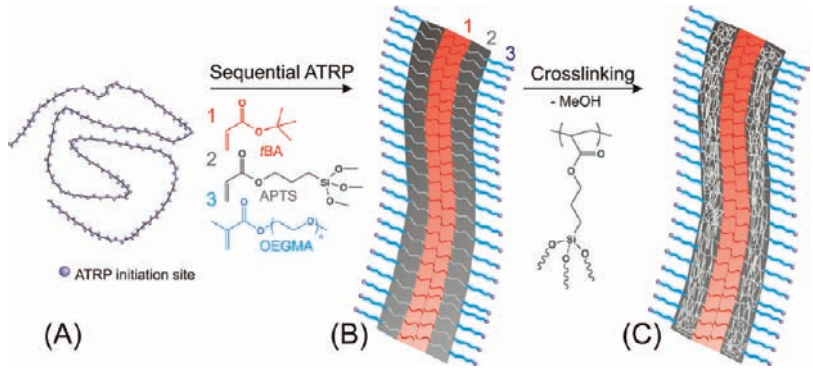

[a] (A) ATRP polyinitiator backbone (PBIEM) with DP ≈ 3200; (B) core−shell−corona structured CPB [tBA$_{75}$-b-APTS$_x$-b-OEGMA$_y$]$_{3200}$; and (C) water-soluble organo−silica hybrid nanotubes [tBA$_{75}$-b-(SiO$_{1.5}$)$_x$-b-OEGMA$_y$]$_{3200}$.

our previous paper.[13] The initiating efficiency of the PBIEM poly(macroinitiatior) backbone toward tBA was determined as 0.65 by cleaving the PtBA side chains and determining their molecular weight by GPC.

The ATRP of APTS for the shell block and OEGMA for the corona block was conducted exclusively in benzene to suppress the hydrolysis and condensation of the trimethoxysilyl groups in the PAPTS shell block.[34] Typically, in a flask equipped with a septum, CuBr, the poly(macroinitiator), and the monomer (APTS or OEGMA) were added in benzene. The mixture was degassed and stirred until complete dissolution of the poly(macroinitiator) and then heated to 110 °C (in the case of APTS) or 80 °C (in the case of OEGMA). Finally, the degassed ligand, *N*,*N*,*N*′,*N*″,*N*″-pentamethyldiethylenetriamine (PMDETA), was injected to start the polymerization, and an initial sample was taken for ^{1}H NMR measurement. The polymerization was monitored by withdrawing samples for ^{1}H NMR measurements. When a desired conversion was achieved, the reaction was quenched by cooling the reaction mixture to room temperature and exposing it to air. The reaction mixture was purified by filtration through a basic alumina column, and by ultrafiltration using benzene as the eluent under nitrogen atmosphere.

Preparation of [(tBA)$_{75}$-b-(SiO$_{1.5}$)$_{115}$-b-(OEGMA)$_{150}$]$_{3200}$ Hybrid Organo−Silica Nanotubes. 400 mg of [tBA$_{75}$-APTS$_{115}$-OEGMA$_{150}$]$_{3200}$ core−shell−corona CPBs in 200 mL of 1,4-dioxane was mixed with 20 mL of a 25% aqueous solution of ammonia. The reaction mixture was kept under constant stirring at room temperature for 5 days to complete the condensation of the trimethoxysilyl groups. The ammonia was largely removed by rotational evaporation at 30 °C, and the resulting solution was purified by dialysis against dioxane.

Characterization Methods. Gel Permeation Chromatography. GPC in THF was conducted at an elution rate of 1 mL/min using PSS SDV gel columns (300 × 8 mm, 5 μm): 10^5, 10^4, 10^3, and 10^2 Å and RI and UV (λ = 254 nm) detection. Poly(*tert*-butyl acrylate) calibration curve was used to calibrate the columns, and toluene was used as an internal standard.

Atomic Force Microscopy. AFM images were recorded on a Digital Instruments Dimension 3100 microscope operated in tapping mode. The samples were prepared by dip-coating from dilute solutions (0.02 g/L) of the polymer brush or hybrid nanotubes solution in dioxane or benzene onto a clean silicon wafer or freshly cleaved mica to form a monomolecular film.

Transmission Electron Microscopy. TEM images were taken on a Zeiss EM EF-TEM instrument operated at 200 kV. A 5 μL droplet of a dilute solution (0.05 g/L) in dioxane or benzene was dropped onto a copper grid (200 mesh) coated with carbon film, followed by blotting the liquid and drying at room temperature for a short time.

Cryogenic Transmission Electron Microscopy. cryo-TEM was conducted by dropping the aqueous dilute solution (0.1 g/L) on a hydrophilized lacey TEM grid, where most of the liquid was removed with blotting paper, leaving a thin film stretched over the grid holes. The specimens were shock frozen by rapid immersion into liquid ethane and cooled to approximately 90 K by liquid nitrogen in a temperature-controlled freezing unit (Zeiss Cryobox, Zeiss NTS GmbH, Oberkochen, Germany). After the specimens were frozen, the remaining ethane was removed using blotting paper. The specimen was inserted into a cryo-transfer holder (CT3500, Gatan, München, Germany) and transferred to a Zeiss EM922 EF-TEM instrument operated at 200 kV. Cryo-TEM samples in organic solvents, such as THF, were vitrified in liquid nitrogen, respectively.

Proton Nuclear Magnetic Resonance. ^{1}H NMR spectra were recorded to determine the monomer conversion on a Bruker AC-300 spectrometer at room temperature in $CDCl_3$.

Results and Discussion

ATRP was employed to graft PtBA-b-PAPTS-b-POEGMA block terpolymer side chains from a PBIEM polyinitiator backbone, along which 3200 ATRP initiating sites were tethered onto each repeating unit.[13] As shown in the general synthetic route in Scheme 1, three monomers, *tert*-butyl acrylate (tBA), (3-acryloxypropyl)trimethoxysilane (APTS), and oligo(ethylene glycol) methacrylate (OEGMA), were sequentially polymerized in anisole or benzene using CuBr/PMDETA as the catalytic system. Finally, the PAPTS shell block of the obtained core−shell−corona structured CPBs was condensed into a silsesquioxane network in the shell.

To confirm the successful introduction of each block into the side chains, ^{1}H NMR spectra were recorded at each block growth step. When tBA was polymerized from the PBIEM polyinitiator backbone, the ^{1}H NMR peaks of PBIEM in Figure 1A completely vanished due to their rather low content (<3%). Instead, the homopolymer CPB [tBA$_{75}$]$_{3200}$ (Figure 1B) showed a characteristic sharp peak at 1.44 ppm, assigned to the protons in the *tert*-butyl groups. The PtBA homopolymer CPBs were then used as the poly(macroinitiator) for the growth of the PAPTS shell. Figure 1C shows the ^{1}H NMR spectrum of the diblock copolymer CPBs [tBA$_{75}$-b-APTS$_{50}$]$_{3200}$. Besides the peak at 1.44 ppm, another intensive peak appears at ~3.5 ppm, indicating the appearance of trimethoxysilyl groups corresponding to the successful growth of the PAPTS block. In the same manner, the block copolymer CPB [tBA$_{75}$-b-APTS$_{50}$]$_{3200}$ was used as poly(macroinitiator) for the ATRP of OEGMA. The intensity of the peak at 3.5 ppm (Figure 1D,E) is enhanced due

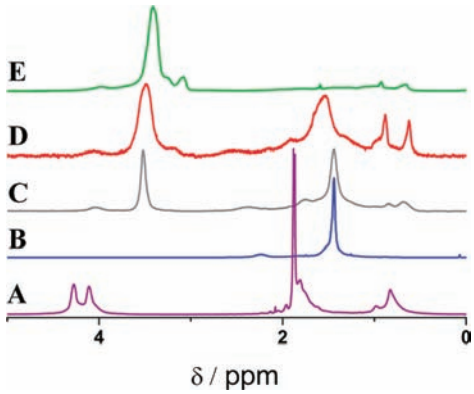

Figure 1. ^{1}H NMR spectra of (A) PBIEM polyinitiator backbone, (B) [*t*BA$_{75}$]$_{3200}$ CPB, (C) [*t*BA$_{75}$-*b*-APTS$_{50}$]$_{3200}$ CPB, (D) [*t*BA$_{75}$-*b*-APTS$_{50}$-*b*-OEGMA$_{30}$]$_{3200}$ CPB, and (E) [*t*BA$_{75}$-*b*-APTS$_{50}$-*b*-OEGMA$_{300}$]$_{3200}$ CPB. All samples were measured in $CDCl_3$.

Table 1. Organo−Silica Hybrid Nanotubes with Different Dimensions[a]

nanotube composition[b]	length[c]	tube diameter[c]	shell thickness[c,d]
*t*BA$_{75}$-*b*-(SiO$_{1.5}$)$_{50}$-*b*-OEGMA$_{300}$	460 ± 120 nm	18 ± 2 nm	∼4 nm
*t*BA$_{75}$-*b*-(SiO$_{1.5}$)$_{115}$-*b*-OEGMA$_{150}$	330 ± 70 nm	27 ± 3 nm	∼10 nm
*t*BA$_{75}$-*b*-(SiO$_{1.5}$)$_{170}$-*b*-OEGMA$_{400}$	285 ± 55 nm	33 ± 3 nm	∼14 nm

[a] Polymethacrylate backbone with 3200 repeating units. [b] After crosslinking. [c] Evaluated from cryo-TEM measurements. [d] Taking into account that the P*t*BA core is always around 8 ± 1 nm.

to the overlapping of the ethylene proton signals of the oligo(ethylene glycol) moieties and those of the trimethoxysilyl groups.

We found the length of the POEGMA block to be very crucial to the success of the synthetic strategy. A short POEGMA corona (DP = 30, ^{1}H NMR in Figure 1D) resulted in an insufficient screening, leading to intermolecular coupling and resulting in large agglomerates that are unstable in solution. Therefore, various terpolymer brushes with a rather long POEGMA corona were synthesized via the "grafting from" approach. After the dialysis of [*t*BA$_{75}$-*b*-APTS$_x$-*b*-OEGMA$_y$]$_{3200}$ from benzene to dioxane, the condensation of the PAPTS shell was carried out by aqueous ammonia. The trimethoxysilyl groups were condensed into a crosslinked silsesquioxane shell. The crosslinked products, [*t*BA$_{75}$-*b*-(SiO$_{1.5}$)$_x$-*b*-OEGMA$_y$]$_{3200}$ organo−silica hybrid nanotubes, are stable in various solvents, like nonpolar benzene and toluene, as well as polar methanol and water. Table 1 summarizes the synthesized organo−silica hybrid nanotubes and their dimensions in aqueous solution.

Molecular visualization via atomic force microscopy (AFM) on mica or silicon wafer has been proven to be a powerful characterization method to verify the successful synthesis and the morphological changes of CPBs.[10,34] Figure 2A−I shows the AFM images of intermediate and final product CPBs at each synthetic step. Figure 2A shows a densely packed monolayer of [*t*BA$_{75}$]$_{3200}$ CPBs with uniform diameter and narrow length distribution. A statistical measurement determines that their average length is 285 ± 74 nm. The cross-section analysis of a single flattened P*t*BA CPB (Figure 2B) shows a height in its center of 1.7 nm (Figure 2C). It is reported that the repulsion among the dense side chains increases with the side chains' length and monomer bulkiness.[1,46,47] Here, by extending the

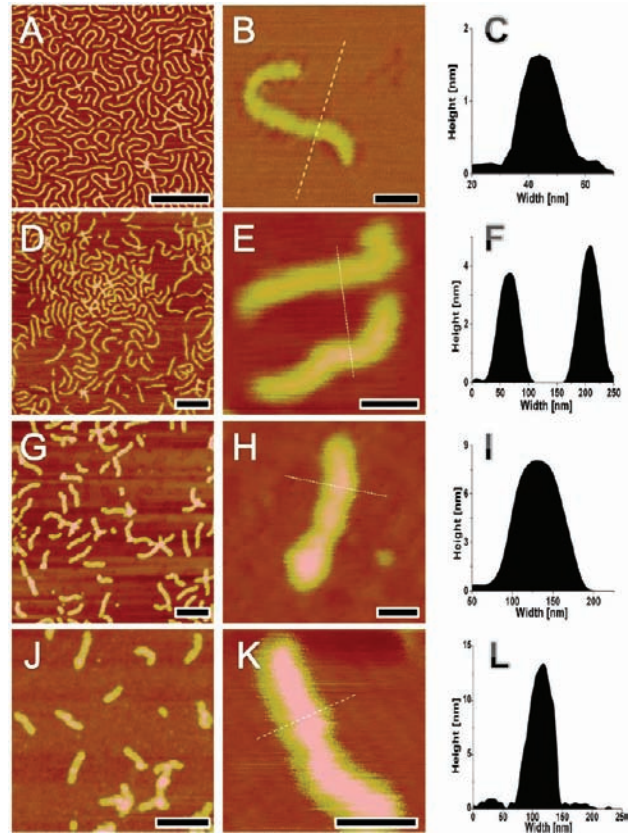

Figure 2. Tapping-mode AFM height images (overview and close view) and the corresponding height cross-section analysis of [*t*BA$_{75}$]$_{3200}$ (A−C), [*t*BA$_{75}$-*b*-APTS$_{115}$]$_{3200}$ (D−F), [*t*BA$_{75}$-*b*-APTS$_{115}$-*b*-OEGMA$_{150}$]$_{3200}$ (G−I), and [*t*BA$_{75}$-*b*-(SiO$_{1.5}$)$_{115}$-*b*-OEGMA$_{150}$]$_{3200}$ (J−L). *Z*-ranges are 5 (A), 8 (B), 9 (D), 10 (E), 15 (G), 20 (H,J), and 25 nm (K), respectively. The scale bars correspond to 500 nm (A,D,G,J) and 100 nm (B,E,H,K), respectively.

side chains by grafting PAPTS as the shell block, the repulsion between the side chains increases as expected. Figure 2D and E shows the AFM images of the diblock copolymer CPBs [*t*BA$_{75}$-*b*-APTS$_{115}$]$_{3200}$. The average length is measured to be 375 ± 50 nm, 30% longer than that of the [*t*BA$_{75}$]$_{3200}$ CPBs. The cross-section analysis of the individual CPBs (Figure 2F) reveals an increase in the height up to 4.5 nm, ca. 200% higher than that of [*t*BA$_{75}$]$_{3200}$. In the absence of a corona block, during the condensation step, the diblock copolymer [*t*BA$_{75}$-*b*-APTS$_{115}$]$_{3200}$ CPBs undergo both intramolecular and intermolecular crosslinking, which precipitates the CPBs out of solution. Thus, a corona block is required to screen the intermolecular coupling before the condensation step and act as a protective layer. Therefore, a POEGMA block with a DP of 150 was grafted (Figure 2G−I) to obtain the final [*t*BA$_{75}$-*b*-APTS$_{115}$-*b*-OEGMA$_{150}$]$_{3200}$ CPB. The average length slightly increased to 400 ± 50 nm. The cross-section analysis revealed a further increase in height to 8.2 nm. The widths (Figure 2 C,F,I) also increased with each polymerization step. However, the wormlike structures appear broader in AFM than in TEM or cryo-TEM measurements due to their spreading on the silicon wafer surface. It is possible to visualize the POEGMA corona with AFM (Figure 2G,H); however, the values for the width of above 150 nm can only derive from the worms being spread out onto the silicon wafer surface.

(46) Linse, P.; Claesson, P. M. *Macromolecules* **2009**, *43*, 2076–2083.

(47) Lee, H.-i.; Pietrasik, J.; Sheiko, S. S.; Matyjaszewski, K. *Prog. Polym. Sci.* **2010**, *35*, 24–44.

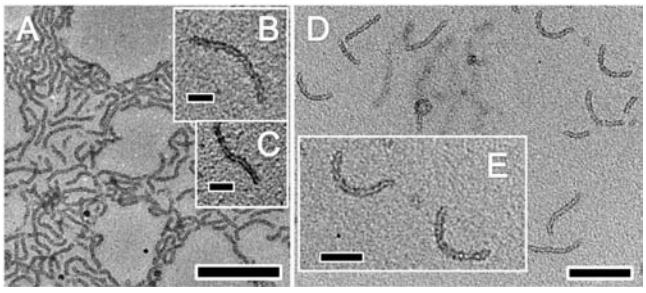

Figure 3. TEM characterization of organo−silica nanotubes in THF: nonstained TEM images of [*t*BA_{75}-*b*-$APTS_{115}$-*b*-$OEGMA_{150}]_{3200}$ (A−C), and [*t*BA_{75}-*b*-$APTS_{170}$-*b*-$OEGMA)_{400}]_{3200}$ (D,E); (B,C,E) are close-ups of nonstained hybrid nanotubes. The scale bars are 100 nm (B,C,E) and 200 nm (A,D), respectively.

As mentioned, the crosslinked product, [(*t*$BA)_{75}$-*b*-$(SiO_{1.5})_{115}$-*b*-$(OEGMA)_{150}]_{3200}$ organo−silica hybrid nanotubes, is stable in various solvents and water. AFM images of the hybrid organo−silica nanotubes are shown in Figure 2J,K. The cylindrical morphology was maintained during the complete synthetic route and actually shaped the silsesquioxane network into a tubular structure. Interestingly, the average length of the cross-linked [*t*BA_{75}-*b*-$(SiO_{1,5})_{115}$-*b*-$OEGMA_{150}]_{3200}$ shrinks from 400 ± 50 to 300 ± 60 nm; meanwhile, their height increases further to 13.2 nm (Figure 2L), ∼60% higher than the precursors (8.2 nm). The longitudinal size contraction and horizontal size expansion result from the intramolecular crosslinking of the side chains. Because more chemical bonds are generated among the side chains in the condensation process, the repulsion force among the side chains is largely compensated. At the same time, both the P*t*BA core and the hybrid silica shell were chemically locked in the CPB center and could not spread over the surface, which enhances the height in the CPB center. Treatment with hydrogen fluoride in THF opens the silsesquioxane network again. Because of the missing crosslinks, the backbone is then able to stretch again. In the case of [*t*BA_{75}-*b*-$(SiO_{1.5})_{170}$-*b*-$OEGMA_{400}]_{3200}$, the average length of the backbone increased from 285 to above 400 nm (see Supporting Information S3).

As AFM measurements only depict the surface morphology, the intrinsic structure of these hybrid nanotubes was revealed by TEM and cryo-TEM measurements. With TEM characterization, nanotubes appear lighter in the center than at the wall, similar to carbon nanotubes. However, for the hybrid organo−silica nanotubes synthesized here, the core is not empty, but filled partially with P*t*BA polymer. Because the polymer has a weak contrast as compared to inorganic or hybrid materials, a tubular structure is thus still expected. In the dry state, the hybrid nanotubes in normal TEM measurements show wormlike morphology (Figure 3), indicating that the cylindrical templates work efficiently for the present synthetic strategy. The nanotubes enlarged in Figure 3B,C,E appear lighter in the core, as expected. The diameters of the core and of the shell of [*t*BA_{75}-*b*-$APTS_{115}$-*b*-$OEGMA_{150}]_{3200}$ in the dry state are 13−17 and 33−37 nm. That gives a wall thickness of ∼10 nm. For the [*t*BA_{75}-*b*-$APTS_{170}$-*b*-$OEGMA_{400}]_{3200}$ nanotubes, the diameter of the core stays around 14−17 nm, whereas the total diameter (core and shell) increases to around 45−54 nm. This results in a shell thickness of approximately 15.5−18.5 nm (in dry state).

As shown above, TEM investigations clearly confirmed the tubular structures. However, the weak contrast of the non-crosslinked organo−silica nanotubes in cryo-TEM measurements in THF made it difficult but possible to depict the tubular structures (Figure 4A). The non-crosslinked nanotubes in aqueous solution were then subjected to cryo-TEM measurements, aiming at detecting the tubular structure in the real solution state (Figures 4B and S1 in the Supporting Information). Crosslinking was a necessity here, because the tubes broke apart otherwise due to strong repellent forces of the corona (see cryo-TEM images in Figure S2). Figure 4 further shows cryo-TEM images of all hybrid nanotubes in water presented in Table 1 (Figure 4C−E). The dark worms represent the crosslinked shell with a P*t*BA core block in its center. Because of the polymer filling inside the tube, the contrast between the core and the wall is weak. Figure 4F shows a single nanotube in water. A gray scale analysis of [*t*BA_{75}-*b*-$(SiO_{1.5})_{115}$-*b*-$OEGMA_{150}]_{3200}$ was performed to precisely differentiate the core and the wall (Figure 4F). Here, the darkest area is located at the wall (yellow/black arrows); the core (red/white arrow) is clearly lighter than the wall but darker than the background. The diameters of the core and the core and shell of [*t*BA_{75}-*b*-$(SiO_{1.5})_{115}$-*b*-$OEGMA_{150}]_{3200}$

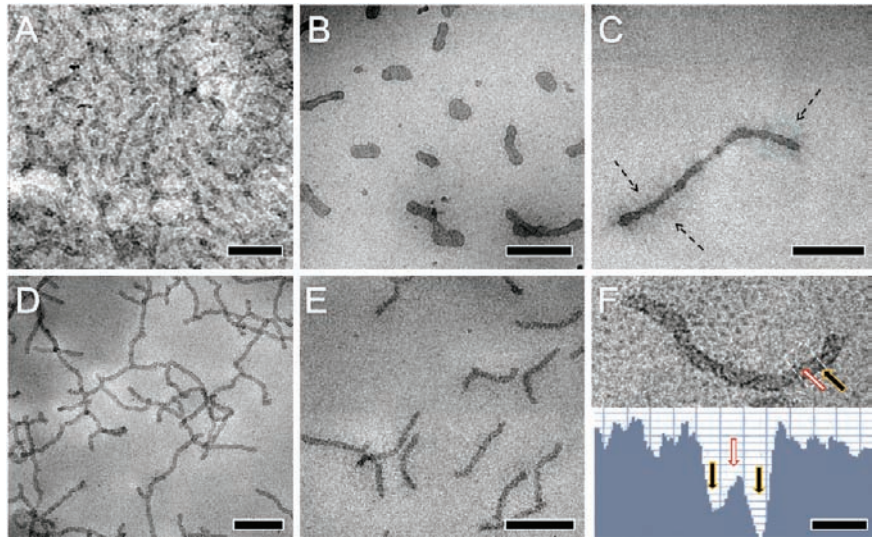

Figure 4. cryo-TEM images of (A) non-crosslinked nanotubes [*t*BA_{75}-*b*-$APTS_{170}$-*b*-$OEGMA_{400}]_{3200}$ in THF; (B) non-crosslinked nanotubes [*t*BA_{75}-*b*-$APTS_{115}$-*b*-$OEGMA_{150}]_{3200}$ in water; (C) hybrid nanotube [*t*BA_{75}-*b*-$(SiO_{1.5})_{50}$-*b*-$OEGMA_{300}]_{3200}$ in water; (D) hybrid nanotubes [*t*BA_{75}-*b*-$(SiO_{1.5})_{115}$-*b*-$OEGMA_{150}]_{3200}$ in water; (E) hybrid nanotubes [*t*BA_{75}-*b*-$(SiO_{1.5})_{170}$-*b*-$OEGMA_{400}]_{3200}$ in water; and (F) a single hybrid nanotube in aqueous solution (the inset is a gray scale analysis of the area shown in image F). The scale bars represent 200 nm (A−E) and 20 nm (F), respectively.

are determined by the gray scale analysis to be 8 ± 1 and 27 ± 3 nm, respectively, again resulting in a shell thickness of ∼10 nm. The diameter of roughly 27 nm does not match the height of crosslinked organo−silica tubes (∼13 nm) in AFM. Although being crosslinked, the tubes are partially flattened out on the substrate, leading to a decreased height and also resulting in a slightly increased width. The corona could not be observed in TEM measurements due to low contrast. Only the cryo-TEM measurement of $[t\mathrm{BA}_{75}\text{-}b\text{-}(\mathrm{SiO}_{1.5})_{50}\text{-}b\text{-}\mathrm{OEGMA}_{300}]_{3200}$ gives slight indication of the corona (Figure 4C, black dashed arrows).

Conclusions

We successfully demonstrated a synthetic route to water-soluble organo−silica hybrid nanotubes templated by core−shell−corona structured triblock terpolymer cylindrical polymer brushes (CPBs). CPBs with a poly(*tert*-butyl acrylate) (P*t*BA) core, a poly(3-(trimethoxysilyl)propyl acrylate) (PAPTS) shell, and a poly(oligo(ethylene glycol) methacrylate) (POEGMA) corona were prepared via the "grafting from" strategy by the combination of anionic polymerization and ATRP. The as-synthesized CPBs then acted as a unimolecular cylindrical template for the in situ fabrication of water-soluble organo−silica hybrid nanotubes via condensation of the PAPTS shell middle block to a silsesquioxane network $(\mathrm{SiO}_{1.5})_x$. With different monomer feed ratios, it was possible to change the dimensions of the formed nanotubes. Not only can the lengths of the nanotubes be controlled rather uniformly by the length of the backbone, but also the actual diameter (P*t*BA and PAPTS) as well as the shell thickness (PAPTS) are easy to adjust. The formed tubular nanostructures were confirmed by transmission electron microscopy (TEM), cryogenic TEM, and atomic force microscopy (AFM). Deprotection of the P*t*BA core to obtain a polyelectrolyte core and the coordination with nanoparticles will be the topic of future research.

Acknowledgment. This work was supported by the Deutsche Forschungsgemeinschaft within the Collaborative Research Center SFB 840.

Supporting Information Available: Cryo-TEM images of non-crosslinked and crosslinked organo−silica nanotubes in aqueous solution and the effect of HF treatment in THF. This material is available free of charge via the Internet at http://pubs.acs.org.

JA107132J